N78-24074

INVESTIGATIONS OF SCALING LAWS FOR JET IMPINGEMENT

J.B. Morton, J.K. Haviland, G.D. Catalano, and W.W. Herling
University of Virginia

SUMMARY

Current developments in upper surface blowing and in externally blown flap configurations have promoted interest in the effects of jet flows on flap or wing surfaces and in the loadings induced on them. The present investigation has been concerned with the scaling laws involved in relating model studies to full-size configurations. As a first step, the statistical properties of tangential flows over surfaces were investigated by two techniques. In one, a laser-Doppler velocimeter (LDV) was used in a smoke-laden jet to measure one-point statistical properties, including mean velocities, turbulent intensities, intermittencies, auto-correlations, and power-spectral densities. In the other technique, free-stream and surface pressure probes connected to 1/8 inch microphones were used to obtain single-point rms and 1/3-octave pressures, as well as two-point cross-correlations, the latter being converted to auto-spectra, amplitude ratios, phase lags, and coherences. The results of these studies supported the vortex model of jets, gave some insights into the effects of surface impingement, and confirmed that jet diameter and velocity are the scaling parameters for circular jets, while Reynolds number is relatively unimportant. Effects of jet Mach number could not be studied due to limitations on flow velocities. Addition investigations were made with a 1/4 scale model of the Langley static thrust stand, with a rectangular nozzle in an upper surface blowing configuration. It was found that there are at least two effective diameters; the one corresponding to the highest frequency peaks in the pressure spectrum appears to be either the hydraulic depth or the minor rectangular dimension. This decays in about five lengths, but does contribute to structural loads. The effective diameter corresponding to the lower peak, which persists for a longer distance, appears to be in agreement with a value given in the literature for far-field noise. There is also some evidence of a third spectral peak at an even lower frequency, corresponding to an effective diameter equal to the major rectangular dimension. Initial surface pressure measurements have been used to obtain dimensionless spectra for comparison with full-scale test data, and agreement has been sufficiently good to support the idea of using low Mach number models for this purpose. However, these spectra are dependent on the acoustical pressure spectra in the nozzle to an as yet undetermined extent, so that it may become necessary to simulate the engine spectra to obtain reliable results.

28

444

PAGE INTENTIONALLY BLANK

INTRODUCTION

The principal goal of this investigation is to determine the scaling laws for the dynamic pressures induced on wing surfaces or flaps of STOL aircraft due to jet impingement. To achieve this goal, the investigators have used an approach which has combined theoretical considerations, basic studies of jet flows, and direct scale model tests on a known configuration. This paper is divided into three sections. The first presents a brief discussion of the literature, and of some of the theoretical considerations which might lead to a method of scaling. The second presents a basic study of the flow in a circular jet blowing over an airfoil surface, using a laser-Doppler velocimeter. The third presents some initial results from a 1/4 scale model of the upper surface blowing facility at Langley, which uses a JT15D-1 engine. Another major effort in this program, now completed (ref. 1), has been an investigation of the flow from a circular jet, which has involved measurement of the fluctuating pressures in the free flow and in the flow impingement on a flat plate.

DISCUSSION

Literature Review

In reviewing the literature, one finds that the single most important contribution to the understanding of jet flows is the replacement of the "classical" jet model shown in figure 1a by the vortex model shown in figure 1b. Early investigators, such as Powell (ref. 2), Bradshaw, Ferris and Johnson (ref. 3), and Mollo-Christensen (ref. 4) had realized that the jet turbulence was structured, while Davies (ref. 5), Crow and Champagne (ref. 6), and Lau, Fisher and Fuchs (ref. 7), to name just a few, contributed to the identification of the vortex structure. Whereas these investigators worked mainly on measuring overall flow statistics, many others attempted flow vizualization. Also, by examining instantaneous signals from pressure transducers, Laufer, Kaplan, and Chu (ref. 8) showed that pairs of vortices tend to coalesce into single vortices, as shown in figure 1b. Recently, Lau and Fisher (ref. 9) have argued the case for the 'probable flow', in contrast to the 'idealized flow', both shown in figure 1b.

It is difficult to construct a satisfactory analytical model of the jet structure. However, Batchelor and Gill (ref. 10) showed that the vortex tube which emerges from a jet is unstable, and that this could trigger the formation of vortices. Widnall and Sullivan (ref. 11) showed that individual vortices are unstable, develop lobes, and ultimately break up. Also, Davies et al. (ref. 12) constructed a computer model in which the vortex tube emerging from the jet was represented by small, closely spaced vortices, and showed that these combine into larger vortices, just as the observed vortex tube instability would indicate.

The vortices present in the jet contribute to the characteristic jet spectrum, which peaks at a Strouhal number (frequency f times jet diameter D divided by jet velocity U_J) of between 0.3 and 0.4, so that one might expect this frequency to show up in the dynamic pressures exerted during impingement. There have been some full-scale studies of the effects of jet engines in externally blown flaps and in upper surface blowing configurations (refs. 13-15), and of small cold jets impinging on flat plates (refs. 1, 16-18), which substantiate this.

Since it is known that far-field radiated jet noise originates in the turbulent jet structure, one might well expect some relationship between the jet noise spectrum and the distribution of vortices in the jet. In fact, the noise spectrum in a stationary jet at about 30° to the axis, where it is a maximum, also exhibits a peak at a Strouhal number of around 0.3. The literature on jet noise is extensive, and a good account of it is given by Stone (ref. 19). It is unfortunate that the accepted method of non-dimensionalizing jet noise is to refer it back to the values obtained at 90° where the spectral peak occurs at a Strouhal number of around 1.0, because there are several examples of spectra for slot nozzles, representing upper surface blowing configurations (refs. 20, 21). These show secondary peaks at much lower Strouhal numbers in the 90° case, but there is no information on how these peaks shift as the angle is reduced to 30°.

Theoretical Considerations

The scaling laws for fluid flows are well-known, and it is quite clear that an adequate job of scaling a jet impingement configuration could be done if the correct Reynolds number and Mach number could be obtained, if the internal noise spectra could be scaled, and if the core air were preheated to produce the correct temperature ratio. Then the spectra of pressure coefficients (i.e., fluctuating pressures divided by jet dynamic pressure) as functions of the Strouhal number would be identical for the model and for the full-scale article. Nevertheless, it is virtually impossible to achieve scaling to this extent. Therefore, let us consider to what extent these hypothetical requirements can be relaxed.

First, consider the Reynolds number. Several investigators have reported no apparent effect of Reynolds number above about 10^4, because, although viscosity may play a part in tripping the initial instability which causes the vortex tube to roll up, subsequent behavior of the jet appears to be dominated by the vortex structure, which causes the potential core to disappear in only five jet diameters.

Second, consider the Mach number. It seems inevitable that, once a Mach number of one is reached in the jet, shock formation phenomena will play some part. However, most investigators into jet noise (see, for example, ref. 19) have reported minimal compressibility effects, although there are kinematic effects which play a part in the correction for angle to the jet axis. Also, a small Mach number dependent effect on pressure coefficients was noted in a full-scale upper surface blowing test (ref. 15).

If the effect of Reynolds number is negligible and the effect of Mach number is minimal, it should be possible to design quite simple scale model tests for the determination of dynamic loads on typical STOL configurations, such as in upper-surface blowing and in blown-flap arrangements. One merely has to design a scale model, and to interpret the results in terms of pressure coefficients referenced to jet dynamic pressure and to Strouhal number.

However, two difficulties remain. First, it is not possible to model a fan jet engine correctly with cold air, unless there is 100% mixing ahead of the exit nozzle, because the different densities of the hot and cold air make it impossible to scale both dynamic pressure (dynamic scaling) and jet velocities (kinematic scaling) at the same time. Second, it may be difficult to scale internal engine noise spectra adequately.

LASER VELOCIMETER MEASUREMENTS

Discussion

A discussion of the development of LDV techniques for the measurement of instantaneous velocity components in a smoke laden jet is given in reference 22. Using these techniques, the following can be found; mean velocity components, turbulence intensities, velocity auto-correlations, and velocity power-spectral densities. Also, the presence or lack of smoke laden air at a given point can be used for intermittency measurements. A light scattering technique is also used to measure concentration of smoke. When this concentration is correlated with velocity, useful information about the structure of the jet can be obtained.

The purpose of the laser-Doppler-velocimeter (LDV) experiment was to determine the effects of an airfoil on the flow field of an axisymmetric jet as well as to study the implications of the vortex model of the near field of a free jet. The positioning of the airfoil relative to the exit plane of the jet in figure 2 corresponds to the upper surface blowing configuration. The arrows are scaled to the local velocity vectors obtained by LDV measurements and can be seen to follow the surface contour.

A jet with a contraction ratio of 14 to 1 over a length of 159 mm and an exit plane diameter of 21.4 mm is used to generate a flat velocity profile at its exit plane. The airfoil is composed of two sections, a flat surface 178 mm wide and 75 mm long, and a curved portion with a radius of curvature of 65 mm sweeping out an arc of 70 degrees. This airfoil is a scaled down model of the actual airfoil surface which had been used in the upper surface blowing investigation at NASA-Langley. The ratio of the dimensions of full-scale configuration to the model used in this investigation is about 12 to 1.

The jet and airfoil were placed inside a 203 mm by 305 mm wind tunnel, where a uniform flow was maintained. The exit Reynolds number of the jet was 22 600 while the ratio of the exit velocity U_J of the jet to that of the parallel secondary flow U_{FS} in the wind tunnel was 5.16 to 1.

Mean Velocities

In figure 3, mean velocity profiles for the longitudinal component are presented for three downstream locations (X/D = 2,3,4) and at one vertical position (Z/D = 0.5) for flow fields with and without flap. The ratio of the local excess velocity, $U - U_{FS}$, to the excess core velocity, $U_J - U_{FS}$, is plotted versus lateral distance, Y/D (non-dimensionalized by the diameter of the jet) from the centerline of the jet, where U_{FS} is the free stream velocity of the wind tunnel flow. Two observations can be made concerning the comparison of the flows. With the airfoil present, there is a noticeable increase in the width of the velocity field at each downstream location. Secondly, the maximum velocity at the centerline (Y/D = 0) of the profiles decays much more rapidly. When X/D equals 4 in the freely expanding coflowing jet, the maximum value of mean velocity has decayed to approximately .95 of its exit plane value. However, with the airfoil surface positioned in the flow field, the ratio, $(U - U_{FS})/(U_J - U_{FS})$, has a maximum of approximately .55.

A comparison of lateral mean velocities V for both flow fields in figure 4 indicates once again an increase in the width of the velocity field with the airfoil present. Also, the maximum value of the ratio, $V/(U_J - U_{FS})$, has approximately doubled when X/D equals 4 and Z/D equals 0.5. Profiles of mean velocity in the vertical direction W for the same downstream location (X/D = 4), but different vertical positions (Z/D = 0.5 and 0.185) are also presented in figure 4. When Z/D equals 0.5, the maximum value of the ratio, $W/(U_J - U_{FS})$, is obtained at the centerline of the profile. This is in contrast to the data presented for Z/D equal to 0.185. In this profile, $W/(U_J - U_{FS})$ remains relatively small and constant in the central region of the velocity field and reaches a maximum when Y/D approximately equals 0.90. This fact might indicate that the jet is rotating or rolling up as it spreads out over the surface of the airfoil.

Turbulent Intensities

The axial and radial distributions of the turbulence intensities in terms of the core velocity $u_{rms}/(U_J - U_{FS})$ are plotted versus radial position at the vertical location where Z/D equals 0.50 in figure 5. Once again examination of the comparative profiles yields two observations. First, with the airfoil present, the turbulent velocity field is significantly wider. Second, the potential core region of the axisymmetric jet is broken up much sooner. The turbulent intensities have actually more than doubled in the central regions of the profiles where X/D equals 3 or 4. Thus, the turbulent velocity field is quite dramatically affected by the inclusion of the airfoil surface in the flow.

Concentration-Velocity Correlation

The concentration-velocity correlation coefficient was also measured in the freely expanding jet. It is defined as follows:

$$r_{u\theta} = \frac{\overline{u\theta}}{u_{rms}\,\theta_{rms}}$$

where u is the fluctuating velocity and θ is the fluctuating part of the concentration, both measured at the same point and time in the flow. The three profiles shown in figure 6 are taken where X/D equals 2, 4 and 8.

The significance of the concentration-velocity correlation is that it indicates how closely the passive admixture field is related to the velocity field as one moves downstream. A zero correlation indicates that the fluctuations in the concentration field are totally independent of the turbulent velocity fluctuations, as is the case for the profile taken where X/D equals 2, near the centerline. Though both θ_{rms} and u_{rms} are small in the potential core, they are not negligible. The existence of θ_{rms} at the exit plane is probably due to imperfect seeding. Out from the centerline of the jet, $r_{u\theta}$ initially becomes negative, then changes sign, and eventually reaches a maximum value at an R/D approximately equal to one half. Vortices, which would entrain "clean" air from outside the jet and would then accelerate the entrained air, would give rise to concentration velocity correlations of the shape shown where X/D equals 2. As the potential core breaks up further downstream, the concentration and velocity fluctuations would become more highly dependent in the center region of the jet, as is the case. Thus, the results shown are entirely consistent with the vortex model.

QUARTER-SCALE MODEL STUDY

Discussion

In the study reported in reference 1, unsteady pressure measurements were made in the free flow of a circular jet and of the surface pressures due to the impingement of this jet on a flat surface. All measurements were made with 1/8 inch (3.2 mm) B & K microphones which were connected by plastic tubing to surface probes or to miniature total or static free-flow probes. Instrumentation included mean total velocity, and rms or 1/3 octave spectra of static pressures. Also, two-point auto- and cross-correlations were obtained which were later converted into power spectra, relative amplitudes and phases, and coherences. Considerable emphasis was placed on the measurements of transfer functions for the probes. Although techniques for correction by computer were demonstrated, the necessary calibration equipment was not available at the time, so that corrections had to be made by hand where necessary.

Measurements made in the circular jet supported the vortex model, and were in general agreement with other results reported in the literature when they were expressed in dimensionless form using the jet diameter and velocity as scaling parameters. No dependency on Reynolds number could be seen, and no attempt was made to determine Mach number effects.

During the investigation of the rectangular jet described in the following paragraphs, frequent comparisons are made with the results on circular jets. One question of particular interest is, what form do the vortices take, and what are their characteristic dimensions?

Test Apparatus

A quarter scale model of the nozzle and airfoil used in test on the static thrust stand at Langl. (ref. 14) was built in order to make a direct evaluation of the use of scaling laws in conjunction with low Mach number models The test apparatus used is shown in figure 7. The scaled nozzle is attached to an adapter section leading from a plenum chamber. Two inlets to the plenum chamber are intended for the core and fan air to simulate the JT15D-1 engine. However, the inner nozzle for the core jet has not been installed to date. Initial testing was carried out with two blowers supplying a pressure of 8.25 cm of water (630 N/m^2) which results in a 32 m/s jet. Later, one of the two mufflers was used with one blower, the other inlet being used for a speaker to provide excitation of the pl chamber. With one blower and muffler, the flow velocity fell to 22 m/.

Instrumentation used was the same as that developed for the earlier circular jet study (ref. 1). Free stream probes were of 1.3 mm outside diameter, with four 0.5 mm holes 12.7 mm from the rounded end. The internal diameter was stepped up to 3.2 mm and connected by up to 3 meters of plastic tubing to the 1/8 inch (3.2 mm) B & K microphones. Surface probes were flush mounted holes, 1.0 mm in diameter. It was necessary to correct for probe respons when measuring spectra, particularly with the 3 m tubing, but this response cancelled out when relative amplitudes, phase lags, and coherences were measured.

Correlation Coefficients

In the previous circular jet study of the variation of the correlation coefficient between a probe on the centerline, and a probe at a radial position R, the correlation was found to drop to a minimum when R/D approached one half, so that the probe was behind the jet lip, and then to increase again as R/D increased further. This was attributed to the irregular passage of vortex filaments over the probe when it was located behind the jet lip. The results of a similar study 17 cm behind the exit plane of the rectangular nozzle are shown in figure 8. One probe was placed as indicated in the figure by "ref", and the second was moved to the positions indicated. When the probe was moved vertically in the direction of the smaller dimension, the correlation coefficient became a minimum behind the lower lip, and then increased beyond it. This behavior, which was accentuated when the airfoil was installed, was taken to indicate that vortex filaments were breaking from the lower lip. When the probe was displaced horizontally, the correlation at a given distance was somewhat less, although it again improved with the airfoil installed. The latter behavior was consistent with the idea that vertical vortex filaments might be passing at random, and that they could be parts of vortices whose dimensions would be of the order of the minor nozzle dimension. Another indication of the

presence of vortex filaments had been found in the circular jet study to be a peak in the rms pressure as the jet was traversed. A similar traverse of the rectangular nozzle (no figure) shows peaks behind the upper and lower lip, except that the peak behind the upper lip disappears when the airfoil is installed. This could be explained in terms of horseshoe vortices attached to the airfoil.

Phase and Coherence Plots

Three phase lag and coherence plots are shown in figure 9 for two of the locations covered in the correlation study, one of them in the free jet with the airfoil removed. The coherence has much the same significance as correlation, except for being frequency dependent. The phase lag is a direct measure of convection velocity between two points. Thus, in the examples shown in figure 9, the small phase lags indicate that the pressure disturbances arrive at the two probes almost simultaneously. It should be noted that the coherence between two vertically displaced probes is much higher with the airfoil present than in the free jet, and also much higher than for two horizontally displaced probes.

Other phase lag plots (not shown) were obtained with the probes displaced axially and were used to calculate convection velocities. It was found that these velocities were between 0.3 and 0.4 of jet velocity up to 100 Hertz, and that they increased to between 0.6 and 0.7 of jet velocity at higher frequencies. In contrast, convection velocities in the circular jet were constant between 0.6 and 0.7 of jet velocity over the entire frequency range. This could be explained on the basis that the lower frequency disturbances in rectangular jets are associated with large vortices which expand outside the jet flow, and therefore convect more slowly. On the other hand, vortices in the circular jets remain equal to the jet diameter.

One-Third-Octave Spectra

The development of 1/3-octave spectra (referenced to jet dynamic pressure) along the jet centerline, both in the free jet and with the airfoil installed, is shown in figure 10. One can interpret the peaks in the spectra as resulting from disturbances at a Strouhal number of 0.3, but related to vortices of a corresponding effective diameter. Thus, with the flow velocity at 30.8 m/s, the 315 Hertz peak, which decays in 200 mm from the exit plane, could relate to an effective diameter of 29 mm, close to the minor nozzle dimension of 42 mm. The 100 Hertz peak, which persists out beyond 300 mm, could relate to an effective diameter of 92 mm. Stone (ref. 19) suggests an effective diameter D_e of

$$D_e = D_a^{0.6}\, D_h^{0.4}$$

where D_a ($\sqrt{4A/\pi}$) is the diameter based on area, and D_h (4A/P) is the hydraulic depth.

In these equations A is the nozzle area, and P is its perimeter. For the 234 mm by 42 mm rectangular nozzle, D_a is equal to 112 mm and D_h is equal to 71 mm, so that D_e works out to be 93 mm, which is consistent with the 100 Hertz peak. A persistent lower peak also observed at 40 Hertz could relate to an equivalent diameter of 231 mm, close to the major dimension of 234 mm, but this peak could also have been tripped by noise known to be present in the plenum chamber.

Jet Excitation

Because it was suspected that some of the disturbances might be induced by blower noise present in the plenum chamber, a muffler was added, and a speaker was installed for excitation of the plenum chamber. The muffler was found to eliminate disturbances above 50 Hertz, but was noisy at 40 Hertz due to the formation of internal vortices by the 152 mm ducts which were used. The alternate muffler, shown in figure 7, eliminated the 40 Hertz noise but was relatively ineffective at higher frequencies.

The results of exciting the plenum chamber at 1/3-octave band center frequencies are shown in figure 11 in decibels referenced to the levels at the exit plane with the blower running to provide an airflow. When the blower was turned off, the measured level at the exit plane was unchanged, indicating that the pressures measured at the exit were purely acoustic. However, as the probe was moved away from the exit, the pressures increased with the blower on while the acoustic pressures dropped with the blower off. This indicated that the pressure disturbances measured in the jet were attached to vortices which had been tripped by acoustic excitation of the plenum. Measured levels were 15 to 20 decibels above background levels. The rate of buildup was greatest at 160 Hertz, corresponding to an effective diameter of 41 mm in the 22 m/s flow, i.e., the minor dimension, as stated before.

Surface Pressure Measurements

One-third-octave surface pressure measurements were made on the 1/4 scale model for comparison with power-spectral density plots of surface pressures on the full-scale article. The effective diameter D_e was chosen as the scaling dimension, because it has already been recommended for far-field noise (ref.18), and because it appears to relate to the most persistent peak in the static pressure spectra. The spectra were non-dimensionalized as follows:

Strouhal No.

$$St = f D_e/U_J$$

Dimensionless spectral density from power spectral density PSD(f)

$$LDPSD(f) = 10 \log_{10} (PSD(f)\ U_J/q^2 D_e) \text{ decibels}$$

where f is the frequency, U_J the jet velocity, and q is the jet dynamic

pressure.

Dimensionless spectral density from 1/3-octave level L_i

$$LDPSD_i = L_i - 10 \log_{10} f_i + 6.4 - 10 \log_{10} (q^2 D_e / p_{ref} U_J) \text{ decibels}$$

where f_i is the 1/3-octave center band frequency, and p_{ref} is the reference pressure for sound pressure level. A table of the values of the relevant scaling dimensions used is given below.

Table of Scaling Dimensions

	D_e (m)	U (m/s)	q (Pascals)
Model	0.0934	21.6	285.8
Full-scale	0.357	277.4 (910 fps)	22 320 (3.237 psi)

Plots of the dimensionless spectral densities are shown in figure 12 for both the model and the full-scale article. Agreement between the two appears to be as good as might be expected in view of the lack of a core nozzle in the model, and in view of the lack of any attempt to scale internal engine noise in the model. The frequenc peaks at the intermediate points are in quite good agreement with the full scale results. Predicted peak frequencies based on the nozzle dimensions, the effective diameter D_e, and the hydraulic depth D_h are shown in the figure.

CONCLUDING REMARKS

Laser Velocimeter Measurements

The investigation of the effect of an airfoil on the flow from a circular jet showed the following: The jet tends to spread faster in the lateral direction along the airfoil. The potential core region is smaller and pulled down towards the airfoil. And turbulent intensities are increased at least for several diameters downstream.

The investigation of velocity-concentration correlations in the free jet gave results that are consistent with the vortex model of the near field.

Quarter-Scale Model Study

The quarter-scale model study resulted in the following conclusions. There is evidence of a vortex-like structure in a free rectangular jet; however, vortices of several dimensions appear to be present, the smaller vortices dying out faster than the larger ones.

For a short distance from the exit, the pressure spectrum peaks at a frequency whose Strouhal number, based on the minor rectangular dimension or on the hydraulic depth, is about 0.3. However, this decays about five of these dimensions downstream, and is replaced by a lower peak which appears to be based on an effective diameter, as defined in the literature for far-field noise (Westley et al., AGARD-CP-113). These peaks are accentuated when excited by a speaker in the plenum chamber. There may be a low frequency peak, based on the major rectangular dimension, but this was not confirmed.

Airfoil surface pressures can be scaled by reducing them to pressure coefficients based on jet dynamic pressure, and the corresponding frequencies can be scaled by reducing them to Strouhal numbers based on any suitable reference length. However, to facilitate comparisons between nozzles of different shapes, it might be better to use the above-mentioned effective nozzle diameter.

Evidence available to date, but not substantiated further in this study, indicates that the effect of jet Reynolds number is negligible, while the effect of Mach number is certainly small, although not well understood at present.

The effect of the internal noise spectrum of the jet engine is probably of sufficient importance that it will have to be accounted for to some extent.

REFERENCES

1. Schroeder, J. C. and Haviland, J. K.: "Fluctuating Pressures in Flow Fields of Jets", NASA TM X-71979 (1976).

2. Powell, Alan: J. Acoust. Soc. Am. 36, 177-195 (1964).

3. Bradshaw, P.; Ferris, D. H.; and Johnson, R. F.: J. Fluid. Mech. 19, 591-624 (1964).

4. Mollo-Christensen, Eric: J. Appl. Mech. 89, 1- (1967).

5. Davies, P. O. A. L.: J. AIAA 4, 1971-1978 (1966).

6. Crow, S. C. and Champagne, F. H.: J. Fluid Mech. 48, 3, 547-591 (1971).

7. Lau, J. C.; Fisher, M. J.; and Fuchs, H. V.: J. Sound Vibr. 22, 4, 379-406 (1972).

8. Laufer, J.; Kaplan, R. E.; and Chu, W. T.: AGARD-CP-131, March (1974).

9. Lau, J. C. and Fisher, M. J.: J. Fluid Mech. 67, 2, 299-337 (1975).

10. Batchelor, G. K. and Gill, A. E.: J. Fluid Mech. 14, 529-551 (1962).

11. Widnall, S. E. and Sullivan, J. P.: Proc. R. Soc. Lond. 332, 335-353 (1973).

12. Davies, P. O. A. L.: AIAA Paper 75-441 (1975).

13. Schoenster, J. A.: "Acoustic Loads on an Externally Blown Flap System Due to Impingement of TF-34 Jet Engine Exhaust", NASA TM X-71950 (1974).

14. Shivers, J. P. and Smith, C. C., Jr.: "Static Tests of a Simulated Upper Surface Blown Jet-Flap Configuration Utilizing a Full-Size Turbofan Engine", NASA TN D-7816 (1975).

15. Mixson, J. S.; Schoenster, J. A.; and Willis, C. M.: AIAA Paper 75-472 (1975).

16. Foss, J. F. and Kleis, S. J.: "The Oblique Impingement of an Axisymmetric Jet", Division of Engineering Research, Michigan State University, Second Annual Report, to NASA Lewis Research Center, December (1972). [Available as NASA CR-134961 AR-2.]

17. Strong, D. R.; Siddon, T. E.; and Chu, W. T.: "Pressure Fluctuations on a Flat Plate With Oblique Jet Impingement", Institute of Aerospace Studies, University of Toronto, Technical Note No. 107, February (1967). [Also NASA CR-839.]

18. Westley, R.; Woolley, J. H.; and Brosseau, P.: "Surface Pressure Fluctuations From Jet Impingement on an Inclined Flat Plate." Symposium on Acoustic Fatigue, AGARD-CP-113, May 1973, pp. 4-1-4-17.

19. Stone, J. R.. "Interim Prediction Method for Jet Noise", NASA TM X-71618 (1974).

20. Reshotko, M.; Olsen, W. A.; and Dorsch, R. G.: "Preliminary Noise Tests of the Engine-Over-the-Wing Concept. I. 30° - 60° Flap Position", NASA TM X-68032 (1972).

21. Stone, J. R. and Gutierrez, O. A.: "Small-Scale Noise Tests of a Slot Nozzle with V-Gutter Target Thrust Reverser", NASA TM X-2758 (1973).

22. Catalano, G. D.; Morton, J. B.; and Humphris, R. R.: "An Experimental Investigation of an Axisymmetric Jet in a Coflowing Airstream". AIAA J., vol. 14, no. 9, Sept. 1976. (To be published.)

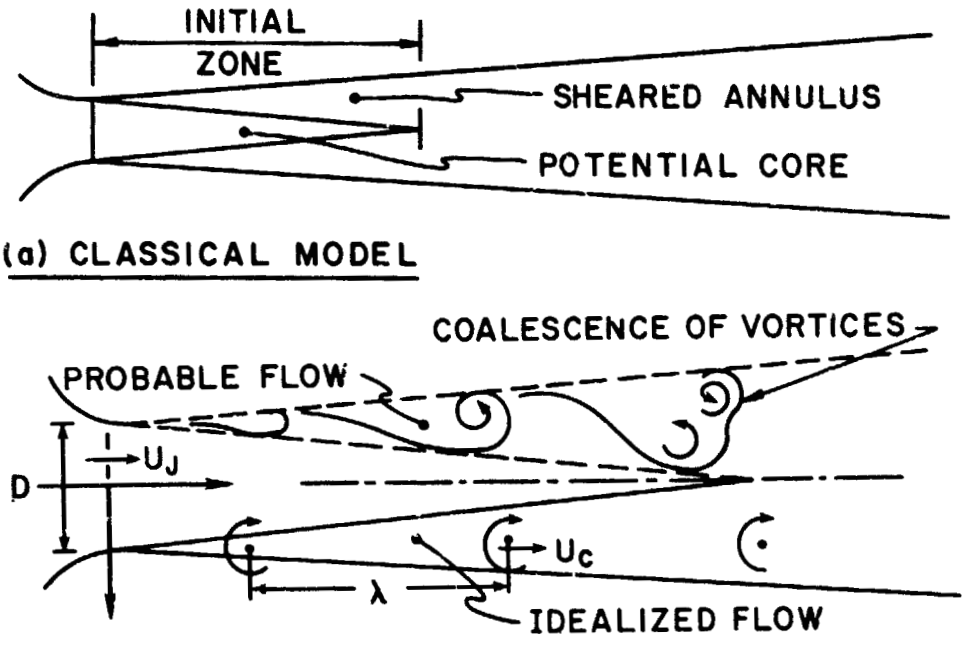

Figure 1.- Current models of the structured turbulence in circular jets. (U_c is the convection velocity of the vortices.)

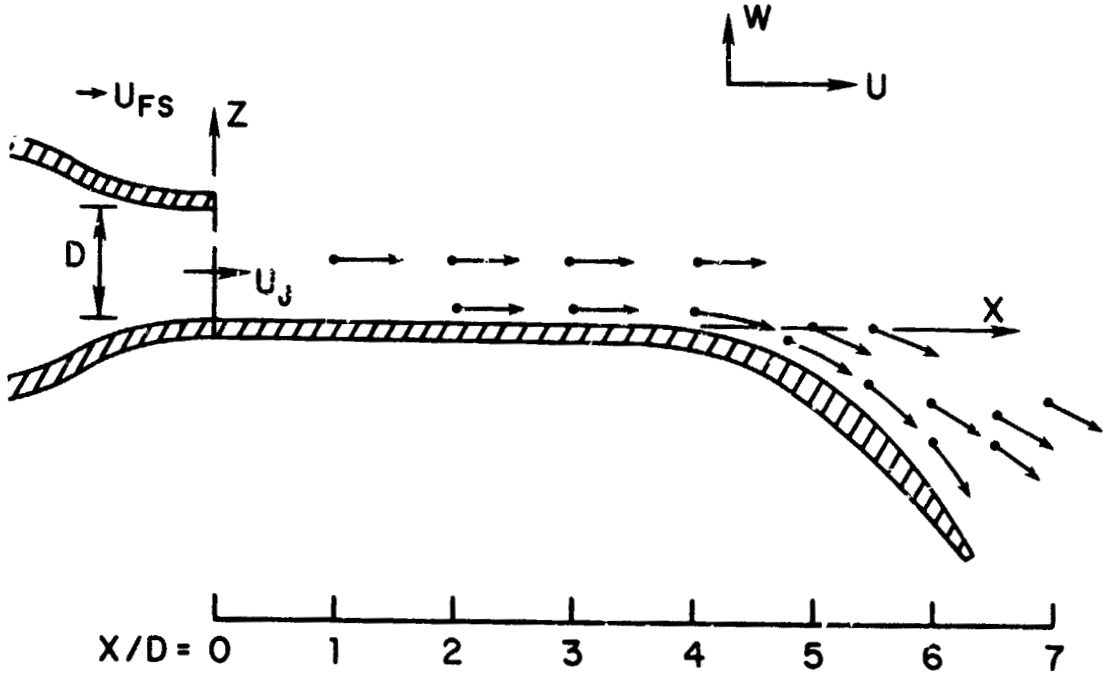

Figure 2.- Vectorial diagram of the mean velocities in the X-Z plane. Circular jet over airfoil, using LDV.

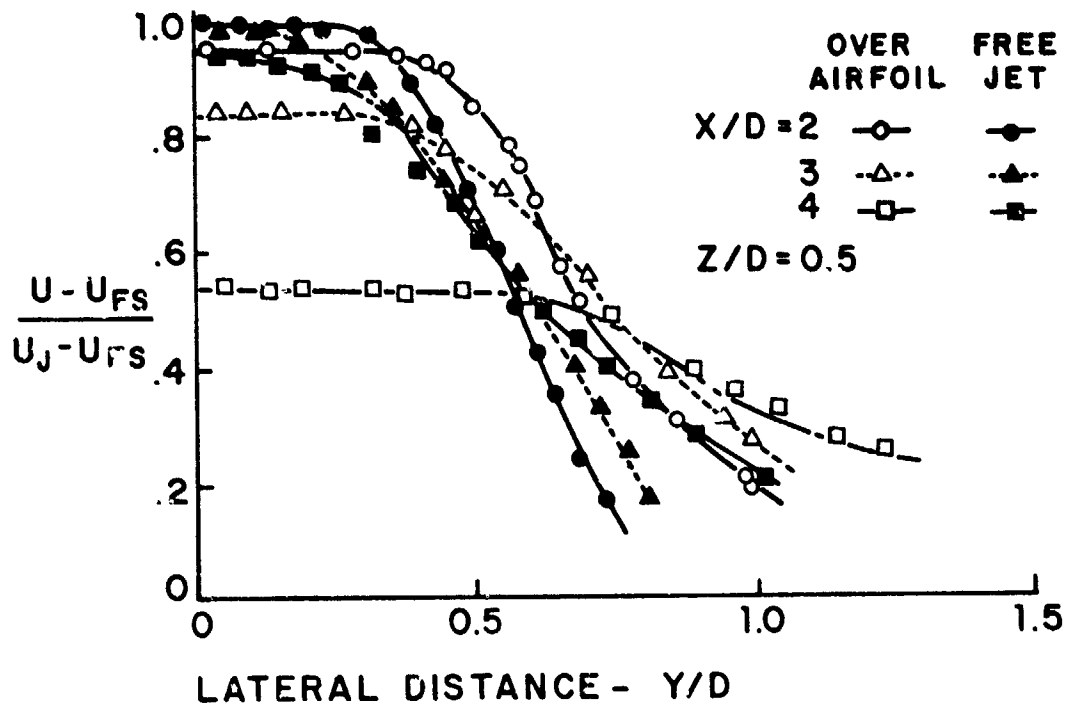

Figure 3.- Profiles of the axial (U) components of the mean velocity. Circular jet over airfoil, using LDV.

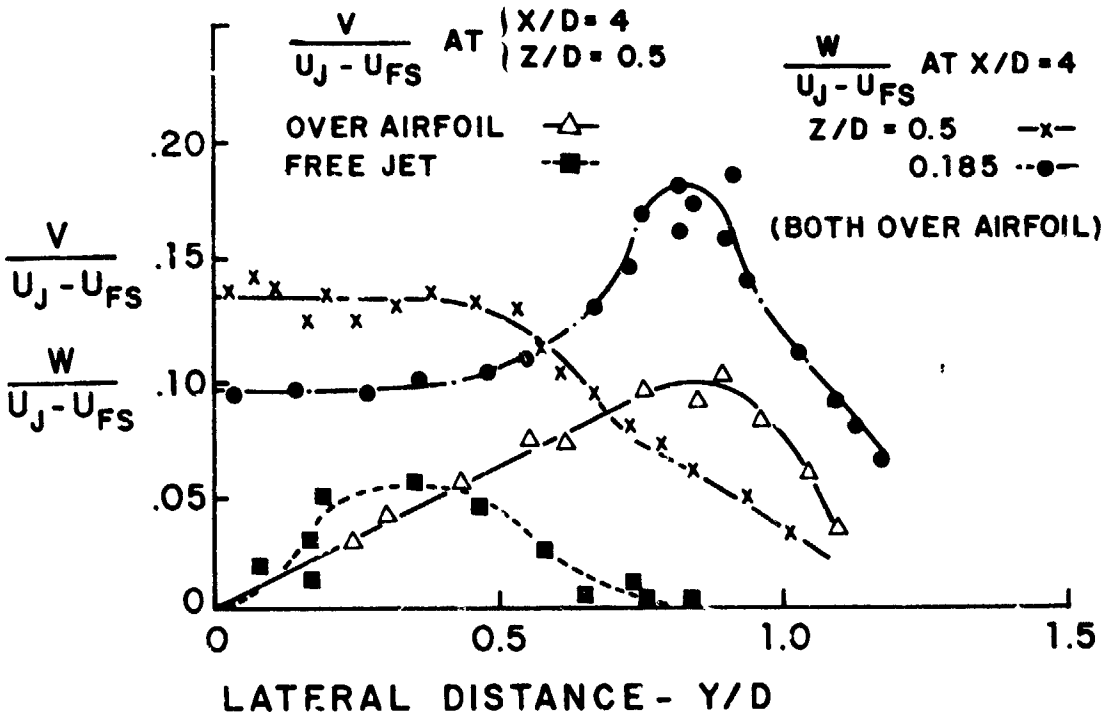

Figure 4.- Profiles of the horizontal (V) and vertical (W) components of the mean velocity. Circular jet over airfoil, using LDV.

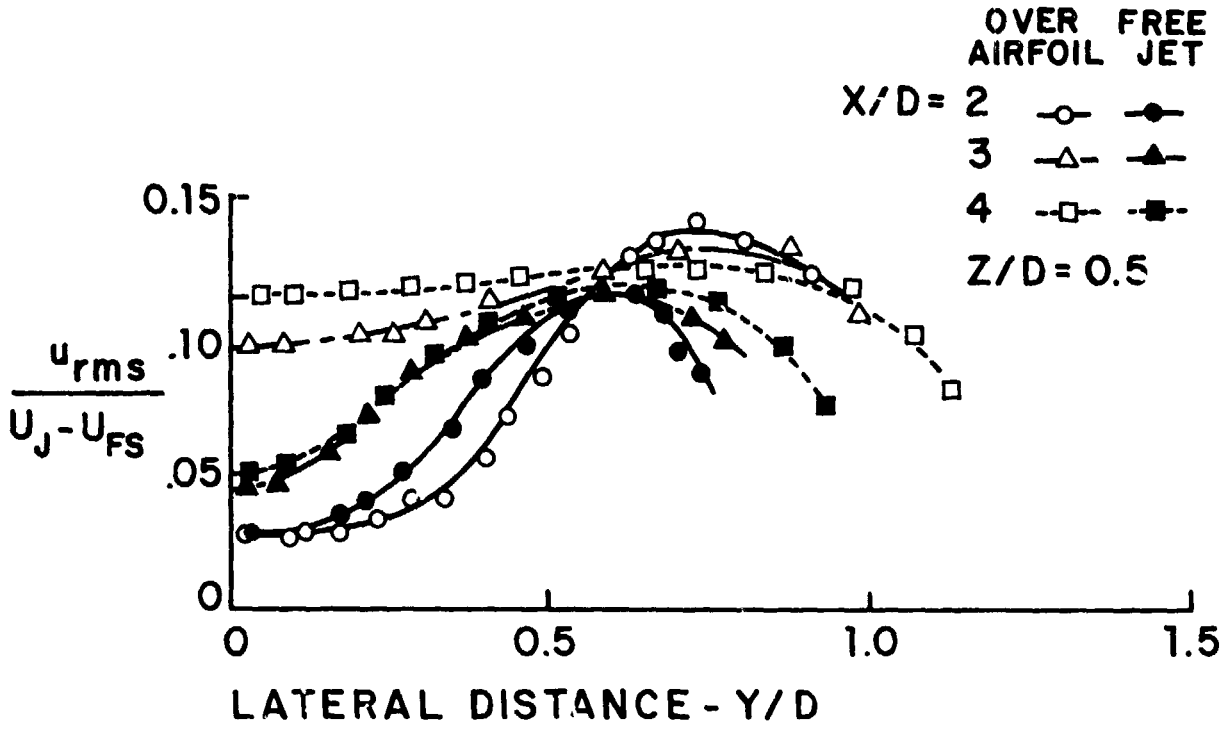

Figure 5.- Profiles of the axial (U) components of turbulence intensity. Circular jet over airfoil, using LDV.

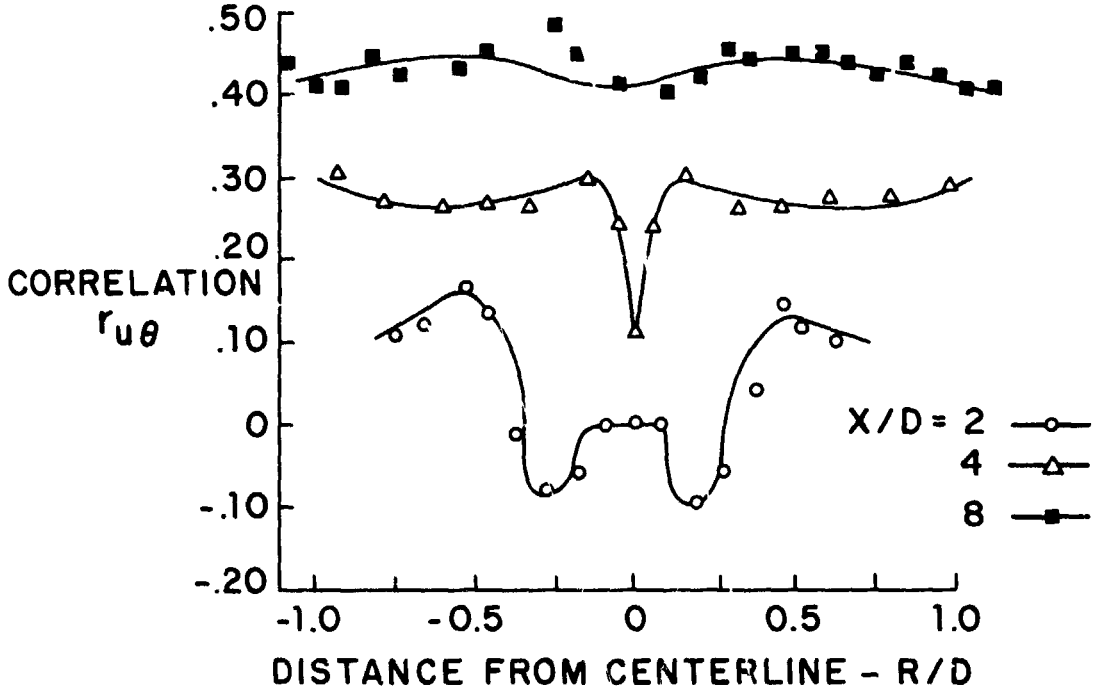

Figure 6.- Profiles of the concentration-velocity correlation coefficient. Free circular jet, using LDV.

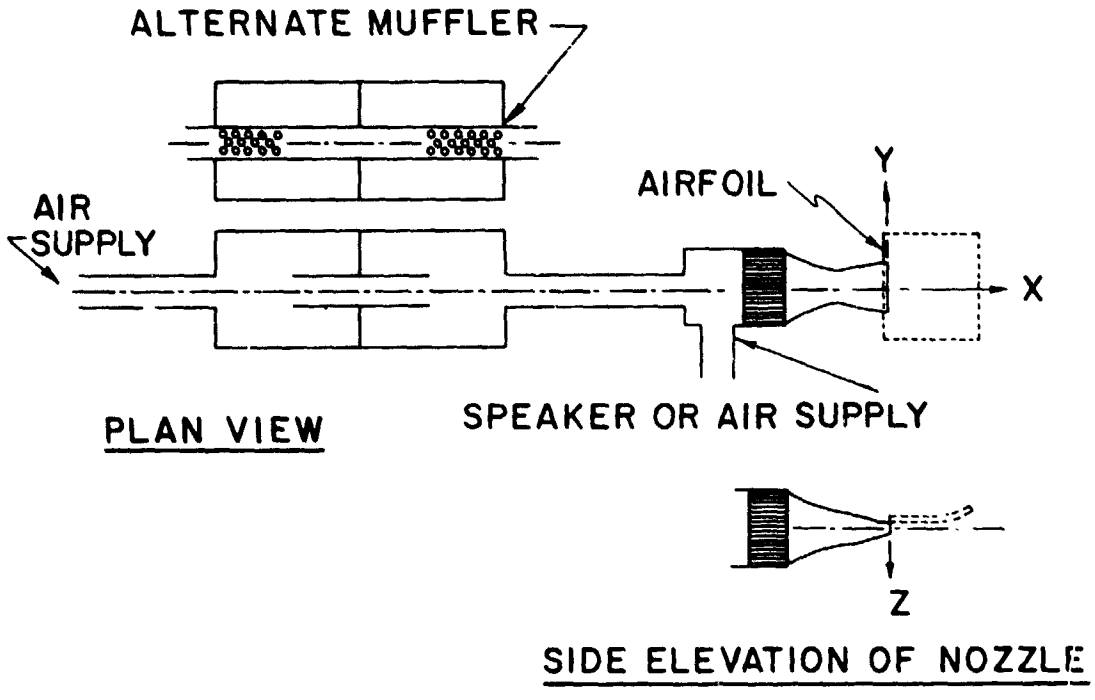

Figure 7.- Schematic of quarter-scale model of upper surface blowing configuration.

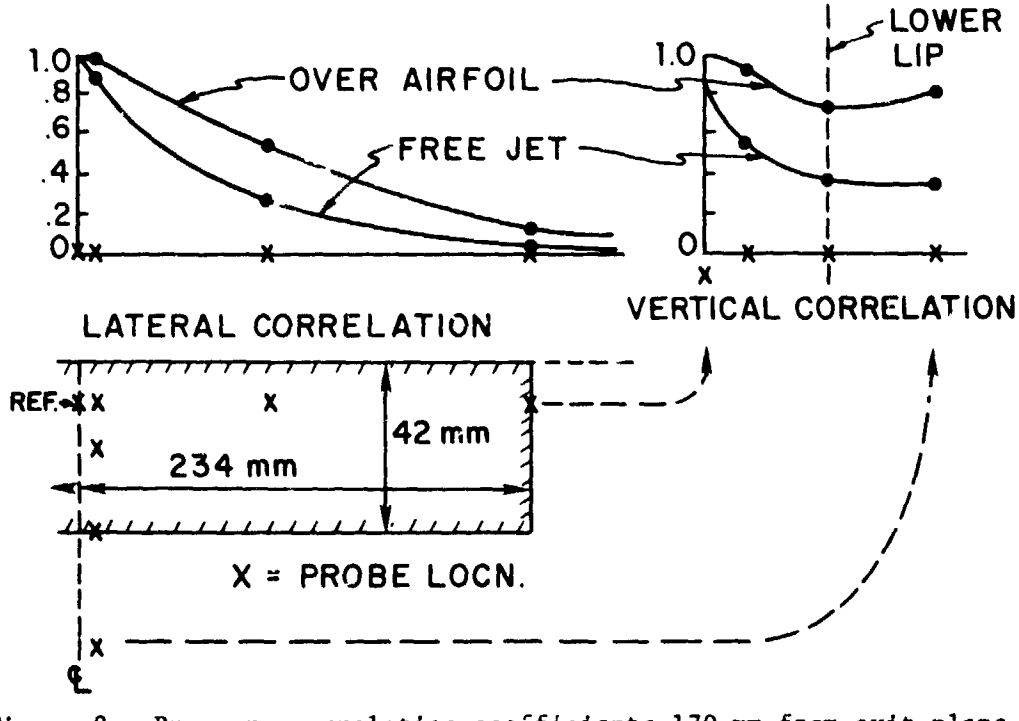

Figure 8.- Pressure correlation coefficients 170 mm from exit plane of quarter-scale model rectangular jet, both free and blowing over airfoil.

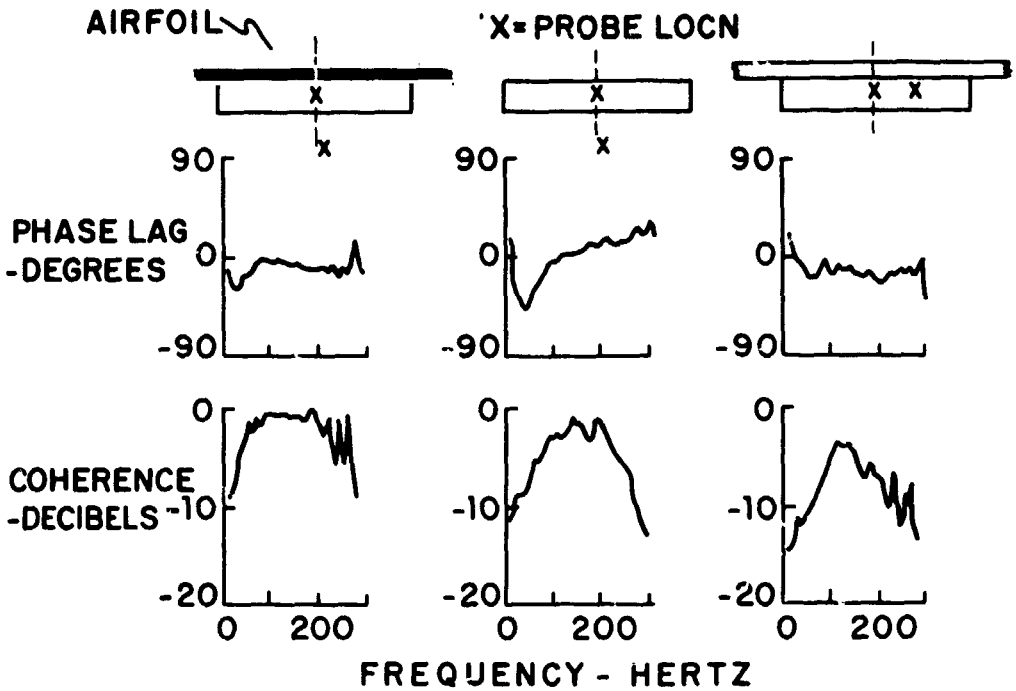

Figure 9.- Phase and coherence plots 220 mm from exit plane of quarter-scale model rectangular jet, both free and blowing over airfoil.

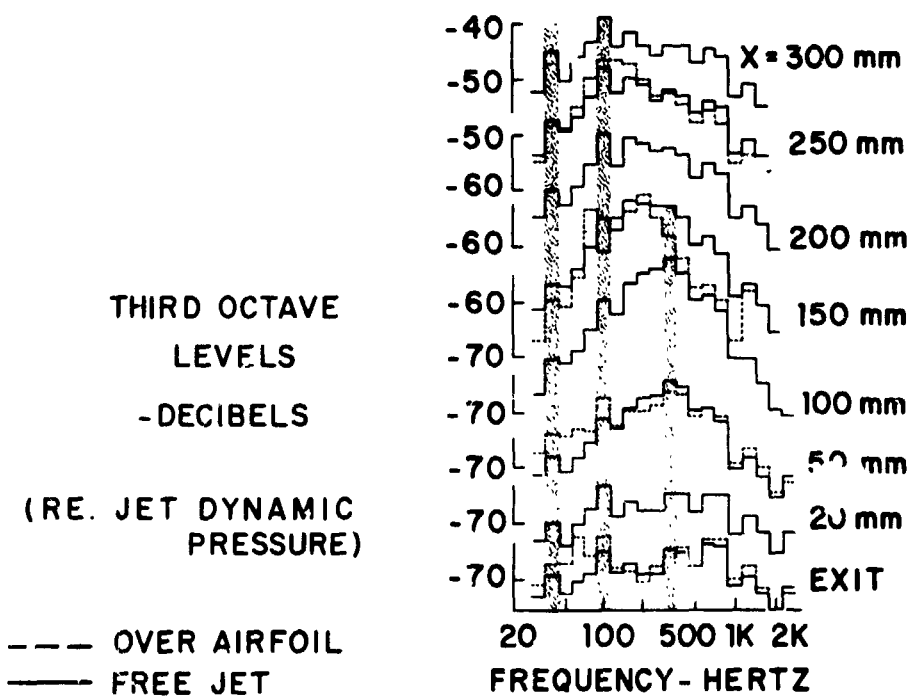

Figure 10.- Growth of 1/3-octave pressure levels in quarter-scale model rectangular jet, both free and blowing over airfoil.

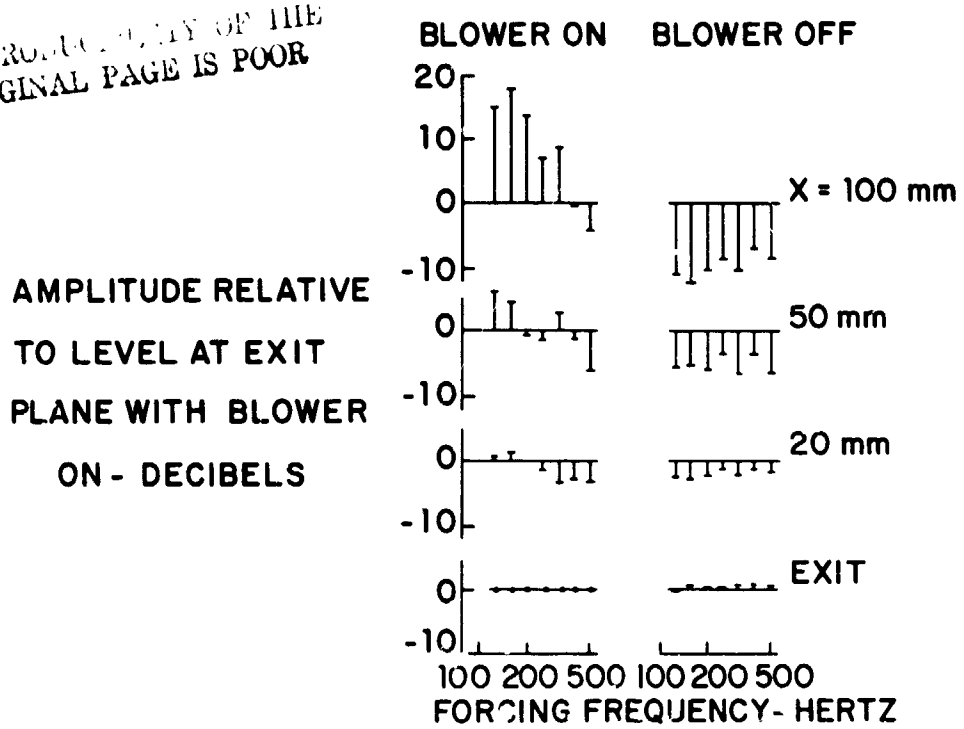

Figure 11.- Effect of forcing separate 1/3-octave band center frequencies in rectangular jet blowing over airfoil, compared with acoustical levels without airflow. Quarter-scale model.

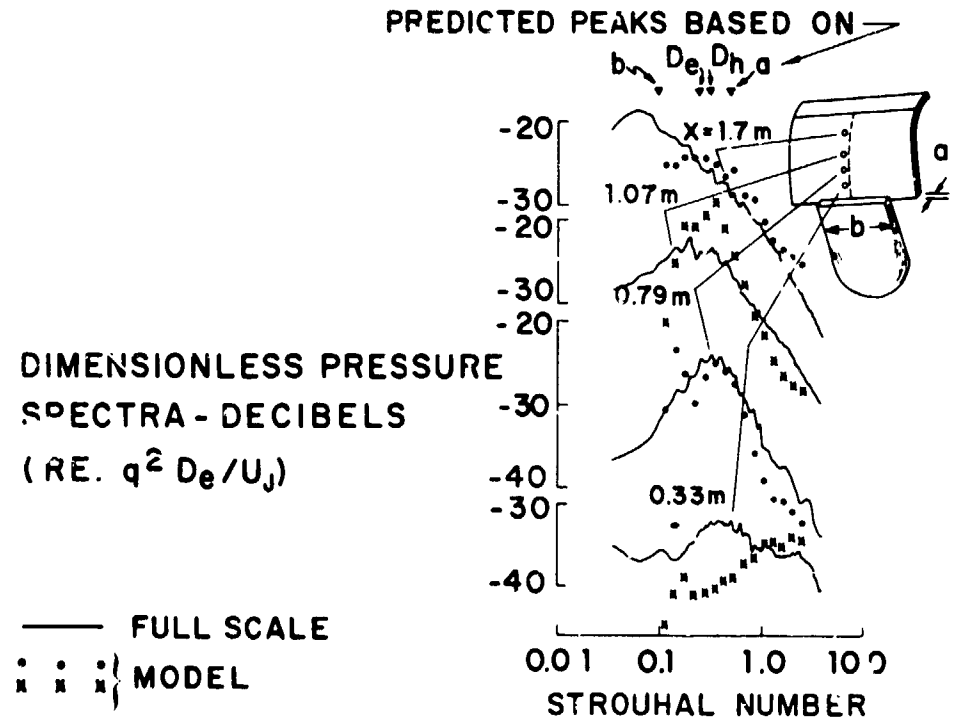

Figure 12.- Comparison of nondimensional power-spectral densities of static pressure spectra. Quarter-scale model vs. full-size configuration.